

W-CVT Continuously Variable Transmission for Wind Energy Conversion System

Claudio Rossi, Piero Corbelli, Gabriele Grandi
Dept. of Electrical Engineering - University of Bologna
Bologna, Italy

claudio.rossi@unibo.it, piero.corbelli@unibo.it, gabriele.grandi@unibo.it

Abstract— This paper investigates the possibility to use a power split electric driven continuously variable transmission as the core of a wind energy conversion system.

The proposed power split transmission for WECS, called W-CVT allows to control the speed of the turbine rotor by keeping constant the speed of the electric generator. The W-CVT is constituted by a planetary gear set integrated with a small size electric machine. This device is installed between the step-up gearbox and a fixed speed fixed frequency electric generator. The limitation of the transmissible torque between the rotor and generator due to the introduction of the W-CVT could be preserve the system components during wind-gusts or electric faults on the grid side. This paper introduces the W-CVT concept, the dynamic model of a complete WECS transmission based on the W-CVT, a design criteria for sizing the CVT and some preliminary results obtained with this system.

I. INTRODUCTION

Wind Energy Conversion System (WECS) is considered one of the most important application of variable speed constant frequency (VSCF) system. The integration of the WECS with the grid requires to generate electric power at constant electrical frequency. The need to maximize the power with wind fluctuating requires regulation of the turbine mechanical speed.

Among the possible combinations of converter, generator, and gearbox for WECS in the power range 100kW - 3MW, the use of a Wound Rotor Induction Generator WRIG coupled to a fixed ratio gearbox represents the most common solution [1]-[6]. Up to now a minor interest seems to be paid to the gearless solutions based on the use of a multipole synchronous

generators. Only few manufacturers of WECS based on Permanent Magnet Synchronous Generators PMSG or Wound Rotor Synchronous Generator WRSG are reported. These direct drive solutions are still very expensive due to the full scale AC/AC converter for the integration with the grid of the generated power [7-10].

WRIG for WECS are based on a 4 or 6 poles machine with stator phases directly connected to the grid, and rotor phases connected through slip rings to a bidirectional power converter. This configuration allows the WRIG to operate both in subsynchronous and supersynchronous conditions. During subsynchronous operation, the rotor absorbs a fraction of the power generated from the stator, whereas during supersynchronous operation both stator and rotor inject power to the grid [11]. In a WRIG if ω_s is the synchronous speed of the generator, and P_{Sr} is the rated power of the stator, a regulation of the generator speed ω in the range $(1-s)\omega_s \leq \omega \leq (1+s)\omega_s$ requires a power rating of the rotor converter $P_R = sP_{Sr}$. Usually the maximum slip is around $s = 0.2 \div 0.3$, and then the sizing of the bidirectional rotor converter is $0.2 \div 0.3P_{Sr}$. For example, assuming $s = 0.3$ (and than $P_R = 0.3P_{Sr}$), it is possible to regulate the speed from 53% to 100% of the maximum speed $\omega_{MAX} = (1+s)\omega_s$. Once the rotor power rating is defined, the current rating of the bidirectional rotor converter is chosen by selecting a proper value of the rotor and stator turn ratio. Usually less turns are put on the rotor side and than a transformer for feeding the rotor converter is required.

This paper deals with a driveline for WECS based on a Continuously Variable Transmission (CVT) placed at the high speed end of the step up gear train. The CVT decouples the variable speed of the gear train output from the fixed (or quasi fixed) speed of the generating machine. In this way the electric generator can be a conventional wound rotor synchronous machine or a squirrel cage induction machine with 4 or 6 pole, directly connected to the grid.

The CVT is constituted by a mechanical differential gearbox integrated with an additional electric machine called driver. A variable speed control of this driver machine allows to adjust the step up ratio of the CVT in a speed range which is larger than that obtained with traditional WRIG drive systems. This solution was proposed for the first time 25 years ago[12], but the early development stage of variable speed drive did not allow to obtain satisfactory results. More recently the use of a

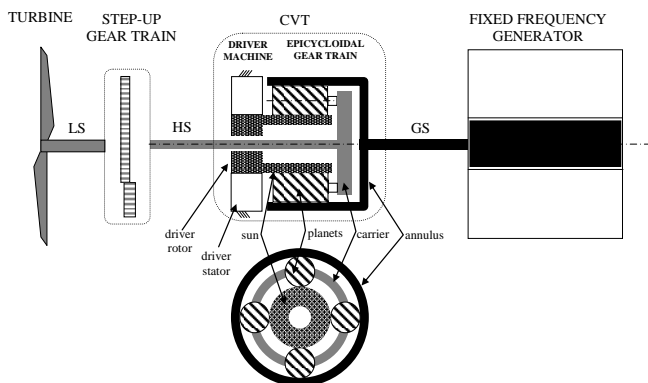


Fig. 1 Scheme of the CVT for WECS

CVT transmission for WECS based on a differential gearbox appeared again [13], [14] but in these cases the transmission is driven by a hydrodynamic system. These hydrodynamic CVTs are based on a complex torque converter, constituted by a variable geometry pump and turbine actuator which drives one element of a differential gearbox. The experience recently gathered with hydrodynamic CVT have demonstrated the possibility to use conventional synchronous or asynchronous generator, and the possibility to smooth the oscillations in the grid injected power through the control of the transmission. Unfortunately, the use of a fluid-machine determines a high level of complexity and decreases the efficiency of the transmission.

A schematic drawing of the CVT presented in this paper is shown in Fig. 1. The CVT is constituted by a planetary gear stage, where the power from the high speed end (HS) of the step up gear train is supplied to the carrier, the output power delivered to the electric generator is taken from the annulus shaft (GS) and the sun is driven by a variable speed electric drive. In this way the sun acts as driver, adjusting the speed ratio between the carrier and the annulus. This configuration can be considered a simplified version of the electric CVT (E-CVT) now widely developed for hybrid vehicles [15]-[20].

In this system the speed control of the driver machine determines the capability to regulate the speed of the turbine across a wide range, by maximizing the power extraction from the wind for wind speed below the rated speed.

In the following Sections a detailed description of the CVT based power transmission of a WECS is given, comprising the dynamic model of the system and a design criteria that emphasizes the minimization of the power and torque rating of the driver machine integrated with the CVT.

II. SYSTEM DESCRIPTION

A. Wind Turbine Characteristic

For analyzing electric generation capabilities of a WECS, wind turbines are usually modelled by using the following relationship between the wind speed and the mechanical power extracted from the turbine shaft [21], [22]

$$P_W = \frac{1}{2} \rho A_r c_p(\lambda, \theta). \quad (1)$$

Where:

- P_W : power extracted from the wind [W]
- ρ : air density [kg/m^3]
- A_r : cross section of the rotor swept area [m^2]
- c_p : power coefficient
- λ : tip speed ratio (ratio between the blade tip speed [m/s] and the upstream wind speed [m/s])
- θ : pitch angle of the blade [deg]

Several numerical representation for $c_p(\lambda, \theta)$ have been given depending on the turbine geometry [23]- [26]. In this paper the approximation and coefficients introduced in [27] have been used. The difference between turbine models are very small and are not relevant for the scope of the paper.

With respect to the wind speed range, in order to optimize energy extraction and to comply with system power rating, a simplified mode of operation of the WECS is the following. In the low wind speed range, from the minimum wind speed to the rated wind speed, the regulation of rotor speed represents the key point in order to optimize the power capture from the

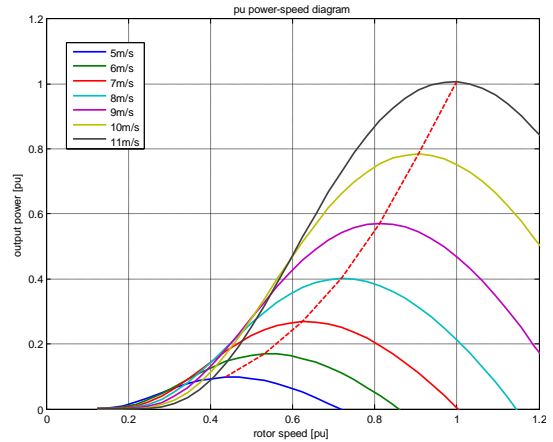


Fig. 2 Power vs. rotating speed, wind speed as parameter

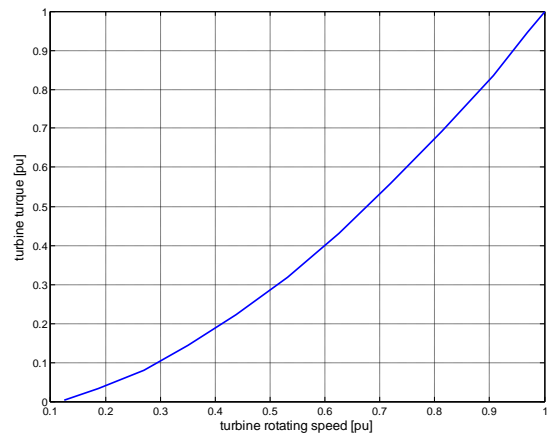


Fig. 3 torque vs. speed at the turbine shaft at MPP

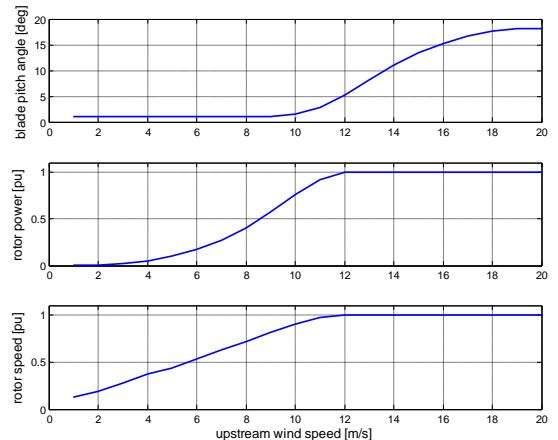


Fig. 4 Blade pitch angle, extracted power at MPP, rotor speed vs. wind speed at MPP

wind. In the high speed range, from the rated wind speed to the maximum wind speed, the WECS should operate at constant rated rotating speed, the blade pitch angle is controlled to cut the wind power from the rotor (pitch to feather or pitch to stall mode) and the system generates the rated power from the generator.

Fig. 2 shows the extracted power vs. rotating speed for a turbine by considering a wind range speed from 5 to 12 [m/s]. In this turbine, for any given wind speed, the maximum power tracking is obtained on the dotted curve.

Assuming the best operation of the maximum power tracking shown in Fig.2 the corresponding mechanical characteristic at the turbine shaft is given by the curve shown in Fig.3. More complex control strategy based on the combination of pitch control and regulation of the rotating speed are often used to smooth the generated power. In these cases the turbine output torque is always below the curve of Fig. 3. By considering the whole operating range of a modern WECS the power curve resulting from an optimal control of the system is represented in Fig. 4b.

B. CVT description

The core of the CVT is the planetary gear set, often referred to also as epicyclic gearing shown in Fig.1. The basic equation to consider in analyzing the quasistatic behaviour of a planetary gear set is the relationship between the speed of the three main parts, which can be derived according to the Willis formula. The planetary gear set can be considered as an ordinary gear set in a rotating frame that is attached to the carrier. Thus, the ratio of the relative speed of the ring and of the sun can be written as

$$\frac{\omega_S - \omega_C}{\omega_A - \omega_C} = \tau_0, \quad (2)$$

where ω_A , ω_S , ω_C , are the speed of annulus, sun and carrier respectively and τ_0 is the epicyclic gear ratio

$$\tau_0 = -\frac{A}{S} \quad (3)$$

where S and A are the number of teeth of sun and annulus respectively.

Fundamental equation for torque in a planetary gear set can be derived from (2) and from power balance yielding to:

$$\begin{aligned} T_S + T_A + T_C &= 0 \\ \frac{T_A}{T_S} &= -\tau_0 \end{aligned} \quad (4)$$

By using (4) the value of torque transmitted to two members of the planetary gear set is given from the torque of the third member.

C. CVT for WECS

In the scheme of the system shown in Fig. 1, the generating machine rotates at constant speed. This case represents the use of a synchronous generator directly connected to the grid, but can be assumed as a good approximation also for a squirrel cage induction generator, because of the very small speed variation due to slip (less than 1% in the MW range).

With reference to the scheme of Fig. 1, the use of the CVT as one stage of the step up gear set is based on the design of the teeth number of the three element of the planetary gear set. This design procedure can be carried out by normalizing the speeds on the basis of the maximum speed of the carrier ω_{Cr} which is given by the characteristic of the turbine and by the gear ratio of the first stages of the step up gear train. The resulting p.u. representation of the three speeds are:

$$\hat{\omega}_C = \frac{\omega_C}{\omega_{Cr}} \quad \text{the speed in p.u. of the carrier}$$

$$\hat{\omega}_A = \frac{\omega_A}{\omega_{Cr}} \quad \text{the constant speed in p.u. of the ring}$$

$$\hat{\omega}_S = \frac{\omega_S}{\omega_{Cr}} \quad \text{the speed in p.u. of the sun}$$

$$\hat{\omega}_{C0} = \frac{\omega_{C0}}{\omega_{Cr}} \quad \text{the speed in p.u of the carrier when the sun is at zero speed } \hat{\omega}_S = 0$$

The relations among the speed of the three elements of the CVT in p.u. is derived from (2) as

$$\omega_S = \tau_0 \omega_A + \omega_C (1 - \tau_0). \quad (5)$$

From (5), the speed $\hat{\omega}_{C0}$ of the carrier, when the sun is at zero speed ($\hat{\omega}_S = 0$), is

$$\hat{\omega}_{C0} = \hat{\omega}_A \frac{\tau_0}{\tau_0 - 1}. \quad (6)$$

Eq. (6) can be used to set the epicyclic gear ratio τ_0 on the base of the required $\hat{\omega}_{C0}$.

By normalizing with respect to maximum torque at the carrier T_{Cr} , the torque in the CVT annulus and solar are given from the torque at the carrier \hat{T}_C by using (2) and (4)

$$\hat{T}_A = \hat{T}_C \left(\frac{\tau_0}{1 - \tau_0} \right) \quad (7a)$$

$$\hat{T}_S = -\hat{T}_C \left(\frac{1}{1 - \tau_0} \right). \quad (7b)$$

The application of the CVT to the WECS is based on the control of the driver speed $\hat{\omega}_S$ in order to keep the generator speed $\hat{\omega}_A$ constant all over the operating speed range of the turbine $\hat{\omega}_C$. In this way, for a given value of the gear ratio τ_0 , the speed required to the driver $\hat{\omega}_S$ is given from (5) as a function of the turbine speed $\hat{\omega}_C$ only, and the torque applied by the turbine to the driver \hat{T}_S and to the generator \hat{T}_A are than calculated from (7).

From the mechanical characteristic $(\hat{\omega}_C, \hat{T}_C)$ of the wind turbine operating in MPPT, represented in Fig. 3, by applying (5) and (7) it is possible to determine torque and power curves in both the driver and the generator.

III. DYNAMIC MODEL OF THE W-CVT TRANSMISSION

A. Epicyclic gearset model

The dynamic equations of the planetary gearbox derive from the relationships between the torques at the gearbox (7), applied at the torque balance equation:

$$T_m - T_{res} = J \frac{d\omega}{dt} \quad (8)$$

For example, the torque transmitted from the carrier to the annulus contributes to accelerate the carrier, to accelerate the annulus, and to contrast the torque at the annulus.

Thus, the annulus equation is:

$$-\frac{\tau_0}{1-\tau_0} T_C = J_A \dot{\omega}_A - T_A - \frac{\tau_0}{1-\tau_0} J_C \dot{\omega}_C \quad (9)$$

where J_A and J_C are the moment of inertia of the annulus and carrier, T_C is the torque applied at the carrier gear, and T_A is the torque applied at the annulus gear. ω_A and ω_C are respectively the annulus and the carrier speed.

Substituting (4) in (9) gives:

$$-\frac{\tau_0}{1-\tau_0} T_C + T_A = J_A \dot{\omega}_A + \left(\frac{\tau_0}{1-\tau_0}\right)^2 J_C \dot{\omega}_A - \frac{\tau_0}{(1-\tau_0)^2} J_C \dot{\omega}_S \quad (10)$$

The solar torque balance at the solar gear is given by:

$$\frac{1}{1-\tau_0} T_C = J_S \dot{\omega}_S - T_S + \frac{1}{1-\tau_0} J_C \dot{\omega}_C \quad (11)$$

where ω_S is the solar speed.

Applying the Willis formula (5) to (11) yields to:

$$\frac{1}{1-\tau_0} T_C + T_S = J_S \dot{\omega}_S + \left(\frac{1}{1-\tau_0}\right)^2 J_C \dot{\omega}_S - \frac{\tau_0}{(1-\tau_0)^2} J_C \dot{\omega}_A \quad (12)$$

The complete set of equation for describing the dynamic behaviour of the planetary gear is the following:

$$\omega_S = \tau_0 \omega_A + (1-\tau_0) \omega_C \quad (13.a)$$

$$-\frac{\tau_0}{1-\tau_0} T_C + T_A = \left(J_A + \left(\frac{\tau_0}{1-\tau_0}\right)^2 J_C \right) \dot{\omega}_A - \frac{\tau_0}{(1-\tau_0)^2} J_C \dot{\omega}_S \quad (13.b)$$

$$\frac{1}{1-\tau_0} T_C + T_S = \left(J_S + \left(\frac{1}{1-\tau_0}\right)^2 J_C \right) \dot{\omega}_S - \frac{\tau_0}{(1-\tau_0)^2} J_C \dot{\omega}_A \quad (13.c)$$

Positive torques in the equations 13 at the first member means the torque has the sense of carrier rotation, negative torques

are in the opposite sense.

From the equations 13 it is possible to obtain the state space model of the transmission:

$$\dot{\mathbf{x}}(t) = \mathbf{A}\mathbf{x}(t) + \mathbf{B}\mathbf{u}(t) \quad (14)$$

$$\mathbf{Y}(t) = \mathbf{C}\mathbf{x}(t) + \mathbf{D}\mathbf{u}(t)$$

Where \mathbf{x} is the state vector, \mathbf{u} is the input vector, \mathbf{Y} is the output vector.

For the planetary drive train the three vectors are defined as:

$$\mathbf{x} = [\omega_A \quad \omega_S]^T$$

$$\mathbf{Y} = [\omega_A \quad \omega_S \quad \omega_C]^T$$

$$\mathbf{u} = [T_A \quad T_S \quad T_C]^T \quad (15)$$

By compacting the inertia coefficient in 13 as:

$$J_{AC} = J_A + J_C \left(\frac{\tau_0}{1-\tau_0}\right)^2 \quad (16a)$$

$$J_{SC} = J_S + J_C \left(\frac{1}{1-\tau_0}\right)^2 \quad (16b)$$

$$J'_C = -J_C \left(\frac{\tau_0}{1-\tau_0}\right)^2, \quad (16c)$$

the equations (13a) and (13b) become:

$$\begin{pmatrix} J_{AC} & J'_C \\ J'_C & J_{SC} \end{pmatrix} \dot{\mathbf{x}}(t) = \begin{pmatrix} 1 & 0 & -\frac{\tau_0}{1-\tau_0} \\ 0 & 1 & \frac{1}{1-\tau_0} \end{pmatrix} \mathbf{u}(t) \quad (17)$$

The matrices \mathbf{A} , \mathbf{B} , \mathbf{C} , \mathbf{D} in (14) are

$$\mathbf{A} = \mathbf{0}; \quad (18a)$$

$$\mathbf{B} = \frac{1}{h} \begin{pmatrix} (1-\tau_0)^2 J_S + J_C & \tau_0 J_C & -(1-\tau_0) \tau_0 J_S \\ \tau_0 J_C & (1-\tau_0)^2 J_A + J_C \tau_0^2 & (1-\tau_0) J_S \end{pmatrix} \quad (18b)$$

where:

$$h = (1-\tau_0)^2 J_A J_S + J_C (J_A + \tau_0^2 J_S)$$

$$\mathbf{C} = \begin{pmatrix} -\frac{\tau_0}{1-\tau_0} & \frac{1}{1-\tau_0} \end{pmatrix} \quad (18c)$$

$$\mathbf{D} = \mathbf{0}; \quad (18d)$$

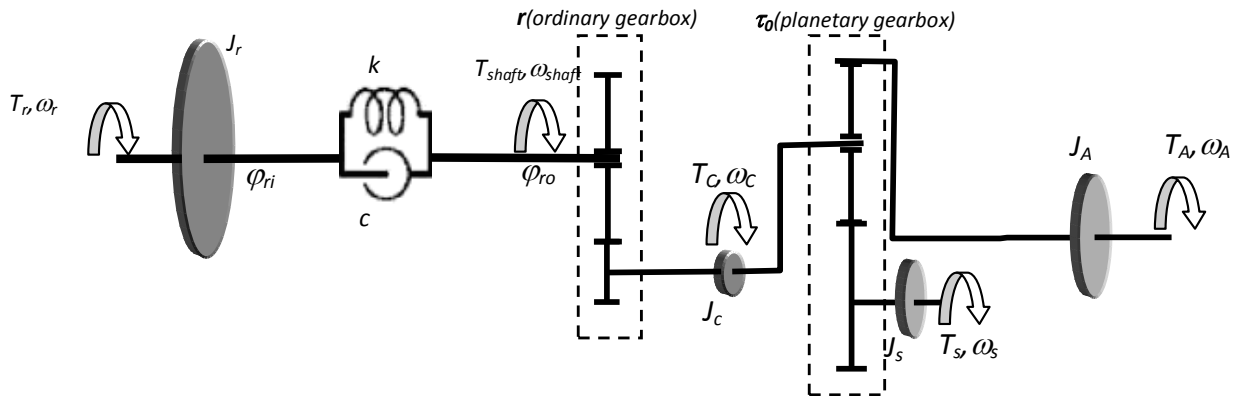


Fig. 5 – WECS drive train with CVT

B. Complete transmission model

The complete WECS transmission is modelled using the so-called ‘‘two mass model’’ which keeps into account the torsion effects for the low speed shaft only. Infinite stiffness can be assumed for the main gearbox and the high speed shaft [28]. Furthermore, the transmission is assumed as ideal, meaning without losses. Using this approximation, the transmission model leads to the following expression for T_C , the torque applied at the carrier shaft of the epicyclic gearbox (high speed shaft):

$$T_C = \frac{1}{r}k(\varphi_{ri} - \varphi_{ro}) + \frac{1}{r}c\left(\omega_r - \frac{\omega_C}{r}\right) \quad (19)$$

while the torque T_{sh} transmitted by the low speed shaft at the step-up gearbox input is:

$$T_{sh} = k(\varphi_{ri} - \varphi_{ro}) + c\left(\omega_r - \frac{\omega_C}{r}\right) \quad (20)$$

Where:

- ω_r is the rotor speed after the hub
- r is the multiplier gear ratio
- ω_c/r is the rotor speed before the multiplier
- φ_{ri} is the low speed shaft angle at rotor hub
- φ_{ro} is the low speed shaft angle at the input of the step-up gearbox
- k is the low speed shaft stiffness coefficient
- c is the low speed shaft damping coefficient

The torque balance for the low speed shaft, and hence for the turbine rotor, is the following:

$$T_r - T_{sh} = J_r \dot{\omega}_r \quad (21)$$

where:

- T_r is the aerodynamic torque at the input of the low speed shaft
- T_{sh} is the torque at the input of the step-up gearbox
- ω_r is the speed at the input of the low speed shaft
- J_r is the turbine moment of inertia

The set of equations (19) - (21) determines the dynamic of the drive train: by the imposition of the torques T_r (coming from the aerodynamic model), the torque T_A (by the generator electrical model), and the torque T_S (by the electrical machine on the solar) the speed of the shafts (ω_r , ω_c , ω_A , ω_S) are given. In this way, the state space representation (14) of the complete model of the drive train can be rewritten using the following vectors:

$$\begin{aligned} \mathbf{x} &= [\omega_A \quad \omega_S \quad \omega_r \quad \Delta\varphi_r]^T \\ \mathbf{u} &= [T_A \quad T_S \quad T_r]^T \\ \mathbf{Y} &= [\omega_A \quad \omega_S \quad \omega_r \quad \omega_C]^T \end{aligned} \quad (22)$$

where:

$$\Delta\varphi_r = \varphi_{ri} - \varphi_{ro} = \int \left(\omega_r - \frac{\omega_C}{r}\right) dt \quad (23)$$

is the torsional angle of the main turbine shaft.

The matrices of (14) **A**, **B**, **C**, **D** have the following expressions:

$$\mathbf{A} = \begin{bmatrix} -\frac{cJ_S\tau_0^2}{hr^2} & \frac{c\tau_0J_S}{hr^2} & \frac{c\tau_0J_S}{hr}(\tau_0-1) & \frac{k\tau_0J_S}{hr}(\tau_0-1) \\ \frac{c\tau_0J_A}{hr^2} & -\frac{cJ_A}{hr^2} & -\frac{cJ_A}{hr}(\tau_0-1) & -\frac{kJ_A}{hr}(\tau_0-1) \\ \frac{c\tau_0}{rJ_r(\tau_0-1)} & -\frac{c}{rJ_r(\tau_0-1)} & -\frac{c}{J_r} & -\frac{k}{J_r} \\ \frac{\tau_0}{r(\tau_0-1)} & \frac{1}{r(\tau_0-1)} & 1 & 0 \end{bmatrix} \quad (24a)$$

$$\mathbf{B} = \begin{bmatrix} \frac{J_C + (1-\tau_0)^2J_S}{h} & \frac{\tau_0J_C}{h} & 0 \\ \frac{\tau_0J_C}{h} & \frac{J_C\tau_0^2 + (1-\tau_0)^2J_A}{h} & 0 \\ 0 & 0 & \frac{1}{J_r} \end{bmatrix} \quad (24b)$$

$$\mathbf{C} = \begin{bmatrix} 1 & 0 & 0 & 0 \\ 0 & 1 & 0 & 0 \\ 0 & 0 & 1 & 0 \\ -\frac{\tau_0}{1-\tau_0} & \frac{1}{1-\tau_0} & 0 & 0 \end{bmatrix} \quad (24c)$$

$$\mathbf{D} = \mathbf{0} \quad (24d)$$

C. Electric machines model

The driver has been implemented by using a IPM-SM controlled in maximum torque per current MTC, all over the speed range. The model of the machine in the d-q synchronous reference frame and the optimal flux weakening control technique have been implemented according to [29] - [30].

The electric generator considered in this paper is a squirrel cage induction machine, with the stator phases directly connected to the grid. This machine has been modeled using d-q axis representation written in a stationary reference frame according to [31].

IV. DESIGN CRITERIA

For analyzing torque and power curve at the CVT elements it is necessary to fix the epicyclic gear ratio τ_0 as defined in (2). Two cases have been considered. In this first case study, τ_0 is selected from (6) in order to have $\hat{\omega}_{C0} = 1$, meaning that, when the driver is at zero speed $\omega_S = 0$, the speed of the turbine is at its maximum speed $\omega_{Cr} = \omega_{C0}$. In the second case τ_0 is selected from (6) in order to have $\hat{\omega}_{C0} < 1$, meaning that when the driver is at zero speed $\omega_S = 0$, the rotating speed of the turbine is lower than its maximum speed $\omega_{C0} < \omega_{Cr}$.

$$\text{A. } \hat{\omega}_{C0} = 1$$

By considering the condition $\hat{\omega}_{C0} = 1$ and then $\hat{\omega}_A = (\tau_0 - 1)/\tau_0$, the power at the carrier \hat{P}_C , at the annulus \hat{P}_A and at the sun \hat{P}_S , from (6), (7a), (7b) are

$$\hat{P}_C = \hat{\omega}_C \cdot \hat{T}_C \quad (25)$$

$$\hat{P}_A = \hat{\omega}_A \cdot \hat{T}_A = -\hat{T}_C \quad (26)$$

$$\hat{P}_S = \hat{\omega}_S \cdot \hat{T}_S = \hat{T}_C(1 - \hat{\omega}_C) \quad (27)$$

Where \hat{T}_C is given from the turbine characteristic and for this case study is given in p.u. in the diagram of Fig. 3.

The three power curves in p.u. are shown in Fig. 6. The dashed line is the input power at the carrier \hat{P}_C , the blue line is the output power at the ring (generator) \hat{P}_A and the green line is the input power at the sun (driver) \hat{P}_S . From the analysis of (25)-(27) and of Fig. 6 the following consideration are made:

- The generator is sized for the full power $\hat{P}_A|_{MAX} = 1$.

When turbine speed and power are lower than the rated values, the driver increases its speed from zero, by absorbing a fraction of the generated power from the grid.

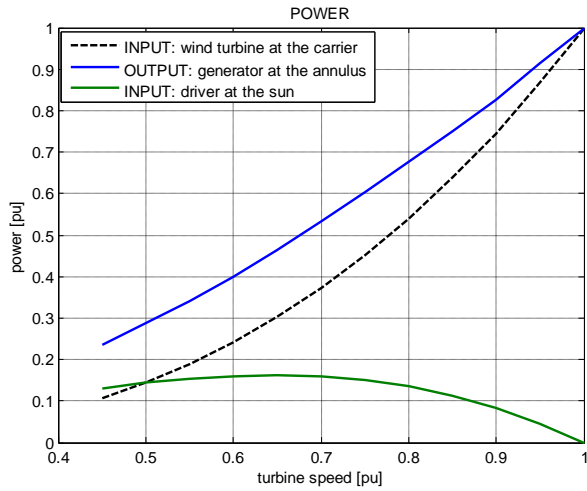


Fig. 6 $\hat{\omega}_{C0} = 1$ Power vs. carrier speed in the three elements of the CVT

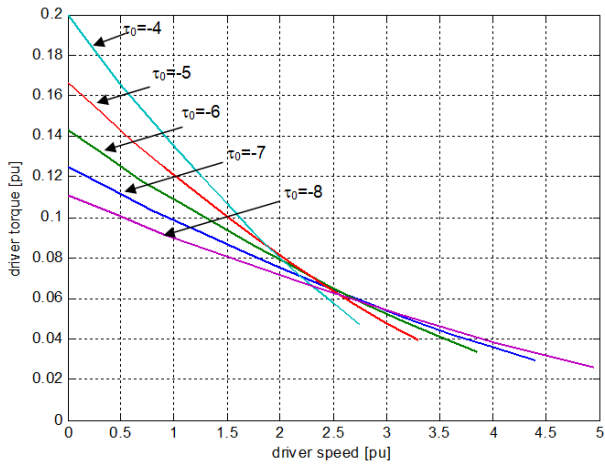


Fig. 7 $\hat{\omega}_{C0} = 1$. Driver torque vs. driver speed for different gear ratio τ_0 of the CVT.

- The driver machine on the sun operates as motor all over the speed range. It means that this drive system is an unidirectional converter.
- The driver power is a small fraction of the turbine power. For the given input $(\hat{\omega}_C, \hat{T}_C)$ curve, the maximum of the driver input power is $\hat{P}_S|_{MAX} = 0.16$. This value represents the power sizing of the power electronic system supplying this machine.
- The power sizing of the driver depends only by Eq. (27). In other words it does not depend from gear ratio τ_0 , and then from the rated speed of the carrier of the CVT. This consideration means that the power sizing of the CVT is the same, regardless of the stage of the step-up gear where it is inserted.

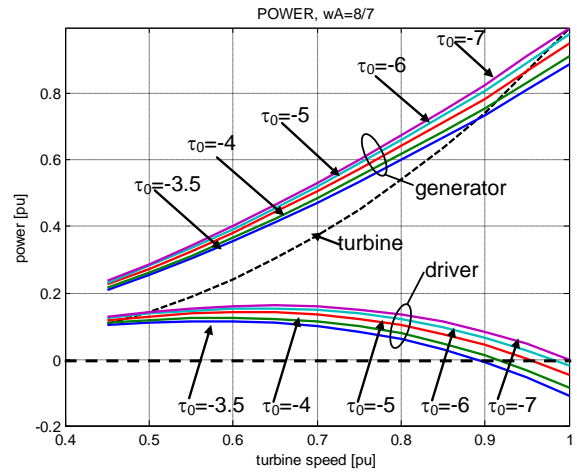


Fig. 8 $\hat{\omega}_{C0} \leq 1$. Power vs. carrier speed in the three elements of the CVT. $\hat{\omega}_A = 8/7$, $\tau_0 = -3.5, -4, -5, -6, -7$

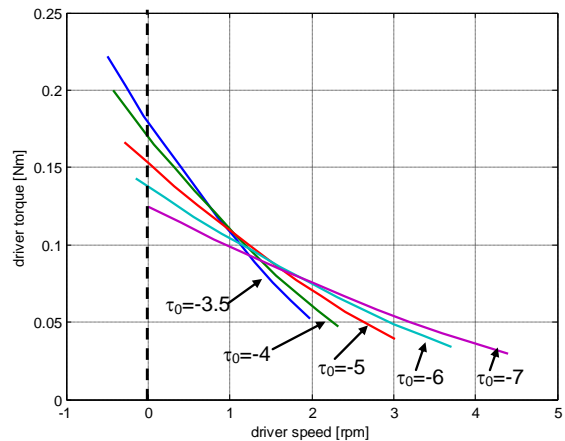


Fig. 9 $\hat{\omega}_{C0} \leq 1$. Driver torque vs. driver speed $\hat{\omega}_A = 8/7$, $\tau_0 = -3.5, -4, -5, -6, -7$

TABLE I
MAIN CHARACTERISTIC OF THE TWO DRIVER CONFIGURATION

	$\hat{\omega}_{C0} = 1$	$\hat{\omega}_{C0} < 1$
minimum driver power $\hat{P}_S _{MAX}$	16%	11%
maximum driver torque $\hat{T}_S _{MAX}$	minimized by the choice of τ_0	always larger than with $\hat{\omega}_{C0} = 1$
generator power $\hat{P}_G _{MAX}$	100%	89%
power converter for the driver	unidirectional	bidirectional (back-to-back)

The capability of the system to regulate the turbine speed at lower values depends on the value of the gear ratio τ_0 , and on the possibility to operate the driver at higher speed. In Fig. 7 is given an example of the required speed-torque characteristic demanded at the driver for several values of τ_0 . In this diagram it is assumed regulation range of the turbine speed $\hat{\omega}_C$ in the range 0.45÷1.

A. $\hat{\omega}_{C0} < 1$

By considering the condition $\hat{\omega}_{C0} < 1$ and then $\tau_0 < 1/(1 - \hat{\omega}_A)$, for a given value of $\hat{\omega}_A$ the power at the carrier \hat{P}_C , at the annulus \hat{P}_A and at the sun \hat{P}_S , are determined directly from the fundamental equation of the CVT (5) and (7) and can be written as follows

$$\hat{P}_C = \hat{\omega}_C \cdot \hat{T}_C \quad (28)$$

$$\hat{P}_A = \hat{\omega}_A \cdot \hat{T}_A = -\hat{T}_C \hat{\omega}_A \frac{\tau_0}{\tau_0 - 1} \quad (29)$$

$$\hat{P}_S = \hat{\omega}_S \cdot \hat{T}_S = -\hat{T}_C \hat{\omega}_C - \hat{\omega}_A \hat{T}_C \left(\frac{\tau_0}{1 - \tau_0} \right) \quad (30)$$

These three power curves in p.u. are shown in Fig. 8 for a given value of the ring (generator) speed ($\hat{\omega}_A = 8/7$) as function of the speed of the turbine $\hat{\omega}_C$ and for different values of the epicyclic gear ratio ($\tau_0 = -3.5, -4, -5, -6, -7$).

The condition $\hat{\omega}_{C0} < 1$, means that the speed of the turbine when the driver is at zero speed is lower than the turbine maximum speed. From Fig. 8 it is clearly shown that the driver operates either as motor for $\hat{\omega}_C < \hat{\omega}_{C0}$ or as generator for $\hat{\omega}_{C0} < \hat{\omega}_C < 1$.

In particular, when the driver operates as generator, both the generator and the driver itself inject power into the grid determining the following main consequences:

- a reduction of the power sizing of the main generator to less than 100% of the rated power of the turbine;
- a reversible power flow in the driver that requires a bidirectional power electronic converter for driver grid interface;
- a reduction of the power sizing of the driver.

TABLE II
CASE STUDY – MAIN PARAMETERS OF THE WECS

Wind Turbine		
rated power	P_R	2 [MW]
rated rotating speed	n_R	18.5 [rpm]
rated wind speed	v_W	12 [m/s]
blade length	b_l	41 [m]
rated power coefficient	C_{PR}	0.3578
tip seed ratio of C_{PR}	λ_i	6.619
pitch angle at rated condition	β_R	2.67 [deg]
pitch angle rate of change	$\dot{\beta}_R$	3[deg/s]
Ordinary step-up gearbox		
low speed shaft inertia	J_{LS}	$5 \cdot 10^6$ [kg·m ²]
gear ratio of the step-up gearbox	r	48.4565:1
low speed shaft stiffness coeff.	k	$5.8 \cdot 10^3$ [Nm/rad/s]
low speed shaft damping coeff.	c	$2.79 \cdot 10^8$ [Nm/rad]
Epicyclic gear train		
epicyclic gear ratio τ_0		-8
gear ratio between the output of the step-up gearbox and the generator with driver stopped ($\omega_S=0$)		1.1255:1
CVT driver: IPM-SM		
rated power	P_{drv}	400 [kW]
rated speed	n_{drv}	1530 [rpm]
rated voltage	V_{LLdrv}	540[V]
pole pairs	p_{drv}	6
inertia	J_{drv}	7[kg·m ²]
stator resistance	R_{Sdrv}	0.045 [pu]
d-axis stator inductance	L_{ddrv}	0.3578 [pu]
q-axis stator inductance	L_{qdrv}	0.6263[pu]
Flux linkage by magnets	Φ_{PM}	0.59 [pu]
Speed range at constant power		1530-3000 [rpm]
Induction generator		
rated power	P_{gen}	2.3 [MVA]
rated voltage	V_{LL}	900 [V]
pole pairs	p_{gen}	3
Rated speed	n_{gen}	1009[rpm]
inertia	J_{gen}	82[kg·m ²]
stator resistance	R_{Sgen}	$0.6156 \cdot 10^{-3}$ [pu]
stator inductance	L_{Sgen}	0.3599 [pu]
mutual inductance	M_{SRgen}	0.2757 [pu]
rotor resistance	R_{Rgen}	$1.145 \cdot 10^{-3}$ [pu]
rotor inductance	L_{Rgen}	0.2757 [pu]
Grid		
Short circuit power	P_{grid}	100 [MVA]
rated voltage	V_{LL}	900 [V]
Transformer short circuit power	P_{SC}	0.07 [pu]
Transformer short circuit voltage	V_{SC}	0.01[pu]

In particular this last features can be seen on Fig. 8 by observing that the minimum power sizing of the driver is obtained with the epicyclic gear ratio $\tau_0 = -3.5$. With this sizing, the maximum power of the driver is about 0.11 p.u. and is reached in motoring mode at a speed 0.6 p.u. and in generating mode at the maximum turbine speed $\hat{\omega}_C = 1$.

Even though the design of the CVT transmission with $\hat{\omega}_{C0} < 1$ is convenient in terms of power sizing both for the generator and the driver machine, this option must be further investigated. For the complete analysis of this case, it is required to calculate the torque demanded at the driver for different values of the epicyclic gear ratio τ_0 . By using Eq. 7b the output torque of the driver is represented in Fig. 9. In this diagram it is shown that when the driver operates in generating mode (for $\hat{\omega}_s < 0$) the maximum demanded torque is increased with respect to the case where the $\hat{\omega}_{C0} = 1$, here represented by the curve $\tau_0 = -7$.

In other words the increase of the torque size of the driver yields to increase the weight of the CVT and then could not probably be accepted, even if accompanied by an under sizing of the main generator.

The relevant aspects of both the design choice: $\hat{\omega}_{C0} = 1$ and $\hat{\omega}_{C0} < 1$ are summarized in Tab.I.

V. SIMULATION RESULTS

A complete model of the WECS has been implemented in a single simulation environment. This model comprises the aerodynamic conversion, the driveline including the CVT, the driver machine, the generator and a simplified grid. A simplified WECS control system have been also developed in order to calculate the reference speed of the driver in any operating condition and the optimal blade pitch angle.

Simulations have been referred to the case study $\hat{\omega}_{C0} = 1$ only. The main parameters of the system subsections have been reported in Tab.II. The driver connected at the sun is an electric drive based on a IPM-SM supplied by the grid, operating over two quadrant only, in motoring mode.

The design condition $\hat{\omega}_{C0} = 1$ is obtained by choosing an epicyclic gear ratio $\tau_0 = -8$, that allows to keep the driver stopped when the turbine rotor is at its rated speed and the output of the step-up gearbox (carrier) is at 896 rpm. When the speed of the rotor decreases due to lower wind speed, the driver is activated and its speed increases. This operation of the driver is characterized by the application of the higher torque at zero speed.

The IPM-SM electric drive used as driver of the CVT satisfy the torque demand at the sun by implementing a mechanical characteristic composed by a speed range operating at constant rated torque T_{drvr} from 0 to n_{drvs} , constant rated power from the rated speed n_{drv} to $2n_{drvs}$, and a speed range operating at decreasing power from $2n_{drv}$ to $4n_{drv}$. Torque overload can reach $2T_{drvs}$, up to a speed corresponding about to $1/2 n_{drv}$. A closed loop regulation system based on a simple PI

regulator has been implemented for the speed control of this electric drive.

The speed reference for the driver is artificially calculated on the bases of the desired speed at turbine shaft for any given wind speed and of the gear ratio. At this early stage of the development no Maximum Power Point algorithm have been yet implemented in the model.

The first test demonstrates the capability of the system to keep constant the generator speed while the turbine shaft speed is changed. This operating mode is typically referred to wind speed below the rated speed. In Fig. 10 is shown that for fast wind speed change (10a), with constant pitch angle (10b), the turbine speed (10c) is regulated by controlling the speed of the driver (10g), while the speed of the generator is almost constant (10e). The torque at the low speed shaft of the turbine (10d) at the generator (10f) and at the driver (10h) are also given. In particular in Fig. 10h the maximum torque that could be applied by the driver to the sun is also given in any operating condition.

The second test demonstrates the capability of the system to limit the transmissible torque between the turbine and the generator. Fig. 11 shows the effect of a sudden gust of wind from 12 to 18 m/s. This wind gust (11a) acts on a turbine rotor with a maximum pitch variation of 3 deg/s (11b). The step increase in the turbine torque (11c) is not transferred to the generator (11f) because of the limitation in the torque that can be applied by the driver (11h). The resulting accelerating torque acts on the turbine rotor speed (11c) and on the driver speed (11g). Acceleration ends as the pitch regulation system cuts the input power and restores the rated turbine speed.

In this condition the limit in the mechanical output torque of the driver acts as a sort of ‘torque limiter’ between the turbine rotor and the generator.

VI. CONCLUSION

A power transmission for WECS based on a Continuously Variable Transmission (CVT) placed at the high speed end of the step up gear train has been presented in this paper. The CVT decouples the variable speed of the gear train output from the fixed (or quasi fixed) speed of the generating machine. In this way the electric generator can be a conventional wound rotor synchronous machine or a squirrel cage induction machine where the power is extract by the stator windings only. A complete model of the CVT integrated in a conventional WECS transmission has been presented. A design criteria underlying the main sizing aspects related to the choice of the epicyclic gear ratio τ_0 of the CVT is also discussed. From this discussion, a solution which minimizes the torque request at the driver and operates the driver only in motoring mode $\hat{\omega}_{C0} = 1$ seems to be preferable.

Some preliminary simulation results have been given in order to confirm the speed regulation capability of this configuration and the possibility to operate the transmission as a torque limiter between the generator and the turbine rotor. This feature, here represented for wind gusts, should also be addressed for fast torque changes at the generator side due to grid faults. This research activity is now under progress

through the realization of a laboratory scale W-CVT prototype.

REFERENCES

- [1] E.S. Abdin, W. Xu, "Control Design and Dynamic Performance Analysis of a Wind Turbine-Induction Generator Unit" IEEE Trans. On Energy Conversion, Vol. 15, No. 1, pp. 91-96, March 2000.
- [2] M.Y. Uctug, I. Eskandarzadeh, H. Ince, "Modeling and Output Power Optimization of a Wind Turbine Driven Double Output Induction Generator," IEE Proc. Electric Power Applications, Vol. 141, No. 2, pp. 33-38, March 1994.
- [3] R. Pena, J.C. Clare, G.M. Asher, "Doubly Fed Induction Generator Using Back-to-Back PWM Converters and its Application to Variable-Speed Wind-Energy Generation," IEE Proc. Electric Power Applications, Vol. 143, No. 3, pp. 231-241, May 1996.
- [4] B. Rabelo, W. Hofmann, "Optimal Active and Reactive Power Control with the Doubly-Fed Induction Generator in the MW-Class Wind-Turbines," Proc. of 4th IEEE International Conference on Power Electronics and Drive Systems, Vol. 1, pp. 53-58, Oct. 2001.
- [5] Z. Chen, E. Spooner, "Wind Turbine Power Converters: A Comparative Study," 7th International Conference on Power Electronics and Variable Speed Drives, No. 456, pp. 471-476, Sept. 1998.
- [6] I. Cadirci, M. Ermis, "Double-Output Induction Generator Operating at Sub-synchronous and Super-Synchronous Speeds: Steady-State Optimization and Wind-Energy Recovery," IEE Proc. B Electric Power Applications, Vol. 139, No. 5, pp. 429-442, Sept. 1992.
- [7] E. Spooner, A.C. Williamson, "Direct coupled, permanent magnet generators for wind turbine applications" Proc. of Electric Power Applications, IEE - Vol. 143, Issue 1, Jan. 1996 Page(s):1 - 8
- [8] M. Popesci, M. V. Cistelecan, L. Melcescu, M. Covrig, "Low Speed Directly Driven Permanent Magnet Synchronous Generators for Wind Energy Applications" Proc. of Int. Conf. on Clean Electrical Power, 2007. ICCEP 07. 21-23 May 2007 Page(s):784 - 788
- [9] L. Hui, C. Zhe "Design optimization and comparison of large direct-drive permanent magnet wind generator systems" Proc. of International Conference on Electrical Machines and Systems, 2007. ICEMS. 8-11 Oct. 2007 Page(s):685 - 690
- [10] A. Binder, T. Schneider, "Permanent magnet synchronous generators for regenerative energy conversion - a survey" Proc. of European Conference on Power Electronics and Applications, 2005 11-14 Sept. 2005 Page(s):10 pp.
- [11] R. Datta, V. T. Ranganathan, "Variable-Speed Wind Power Generation Using Doubly Fed Wound Rotor Induction Machine - A Comparison With Alternative Schemes" IEEE Transactions On Energy Conversion, Vol. 17, No. 3, September 2002
- [12] H. Law, H. A. Doubt, B. J. Cooper, 'Power Control Systems for the Orkney wind-turbine generators' Proc. of Intersociety energy conversion engineering conference; Vol./Issue: 4; 19 Aug 1984; San Francisco, CA, USA
- [13] H. Müller, M. Pöller, A. Basteck, M. Tilscher, J. Pfister, 'Grid Compatibility of Variable Speed Wind Turbines with Directly Coupled Synchronous Generator and Hydro-Dynamically Controlled Gearbox' Proc. of Sixth Int'l Workshop on Large-Scale Integration of Wind Power and Transmission Networks for Offshore Wind Farms, 26-28 October 2006, Delft, NL
- [14] Wikov-Wind W2000 '2MW Wind Turbine' data sheet from Wikov Wind a.s.; www.wikov.com
- [15] S. Matsumoto, 'Advancement of hybrid vehicle technology' Proc. of Power Electronics and Applications, 2005 European Conference on 11-14 Sept. 2005 Page(s):7 pp.
- [16] D. Hermance, "Toyota hybrid system," presented at the SAE TOPTEC Conf., Albany, NY, May 1999.
- [17] Matsuo, T. Miyamoto, H. Maeda, "The Nissan Hybrid Vehicle", SAE Paper 2000-01-1568
- [18] M. Duoba, H. Ng, and R. Larsen, "Characterization and Comparison of two hybrid electric vehicles (HEVs)—Honda insight and Toyota Prius," SAE, Warrendale, PA, Tech. Rep. 2001-01-1335, 2001.
- [19] J. M. Miller, "Hybrid electric vehicle propulsion system architectures of the E-CVT type," IEEE Trans. Power Electron., vol. 21, no. 3, pp. 756-767, May 2006.
- [20] J. Liu, H. Peng, and Z. Filipi, "Modeling and control analysis of Toyota hybrid system," presented at the Int. Conf. Adv. Intell. Mechatron., Monterey, CA, Jul. 2005.
- [21] S. Heier, "Grid Integration of Wind Energy Conversion Systems", 2nd Ed., Wiley, 2006.
- [22] T. Burton, D. Sharpe, N. Jenkins, E. Bossanyi, "Wind Energy Handbook", Wiley, 2001
- [23] O. Wasynczuk, D. T. Man, and J. P. Sullivan, "Dynamic behaviour of a class of wind turbine generators during random wind fluctuations" IEEE Trans. Power App. Syst., vol. 100, pp. 2837-2845, June 1981.
- [24] M. M. Hand and M. J. Balas, "Systematic Controller Design Methodology for Variable-Speed Wind Turbines," National Renewable Energy Laboratory, Tech. Rep. NREL/TP-500-29 415, Feb. 2002.
- [25] N.W. Miller, J. J. Sanchez-Gasca, W.W. Price, "Dynamic modelling of GE 1.5 and 3.6MW wind turbine generators for stability simulations" in Proc. IEEE Power Engineering Society General Meeting, vol. 3, Jul. 2003, pp. 1977-1983.
- [26] A. D. Hansen, C. Jauch, and P. Sorensen, "Dynamic Wind Turbine Models in Power System Simulation Tool Digsilent" Risø National Laboratory, Risø, Denmark, Tech. Rep. Risø-R-400(EN), Dec. 2003.
- [27] J. G. Slootweg, H. Polinder, S. W. H. de Haan, W. L. Kling, "General Model for Representing Variable Speed Wind Turbines in Power System Dynamics Simulations" IEEE Transactions On Power Systems, Vol. 18, No. 1, Feb. 2003
- [28] Henrik Bindner, "Active Control: Wind Turbine Model". Report number: R-920(EN) Risø National Laboratory, Denmark, 1999
- [29] Morimoto, S. Takeda, Y. Hirasa, T. Taniguchi, K. Expansion of operating limits for permanent magnet motor by optimum flux-weakening Proc. of Industry Applications Society Annual Meeting, 1989., Conference Record of the 1989 IEEE , 1-5 Oct. 1989 Page(s): 51 -56 vol.1
- [30] W. L. Soong, T.J.E. Miller: Field-weakening performance of brushless synchronous AC motor drives. Electric Power Applications, IEE Proceedings- , Volume: 141 , Issue: 6 , Nov. 1994 Pages:331 - 340
- [31] Ned Mohan "Advanced Electric drives" MNPERE Minneapolis MN - USA, 2001. ISBN 0-9715292-0-5.

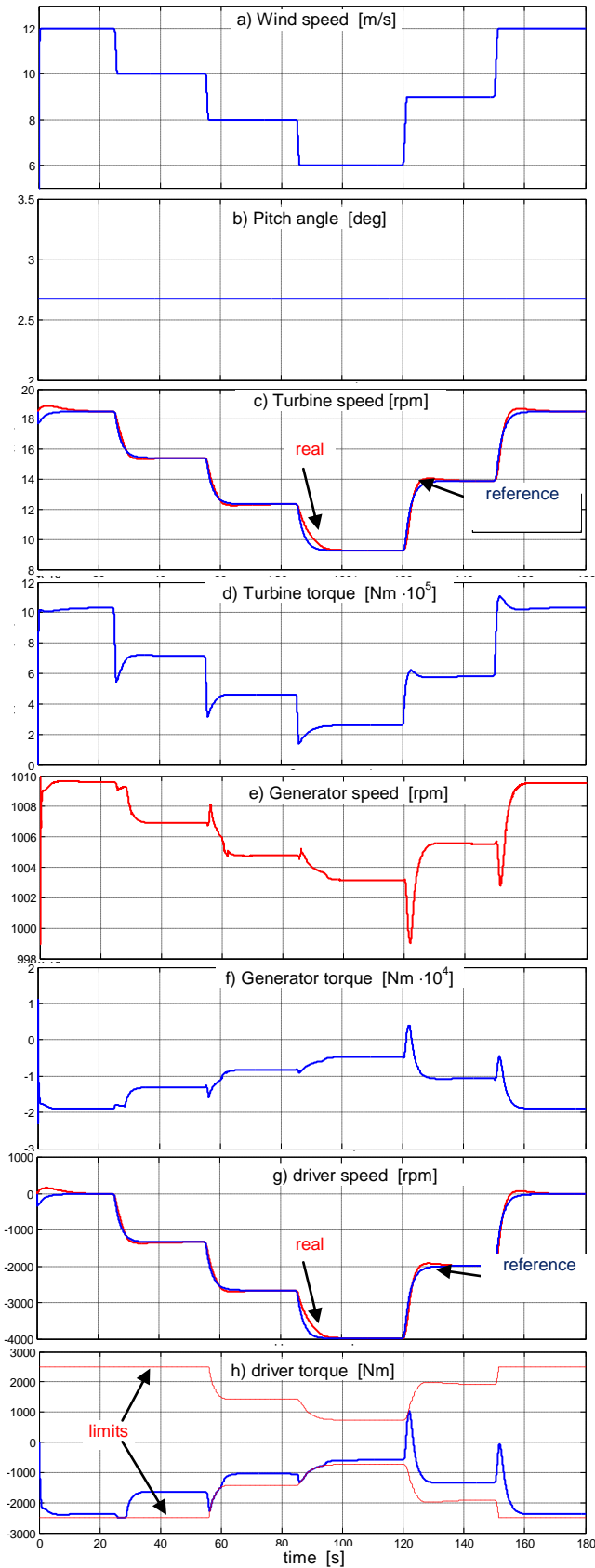


Fig. 10 WECS operation for wind speed below the rated value
 a-d) turbine data; e-f) generator speed and torque; g-h) driver speed and torque.

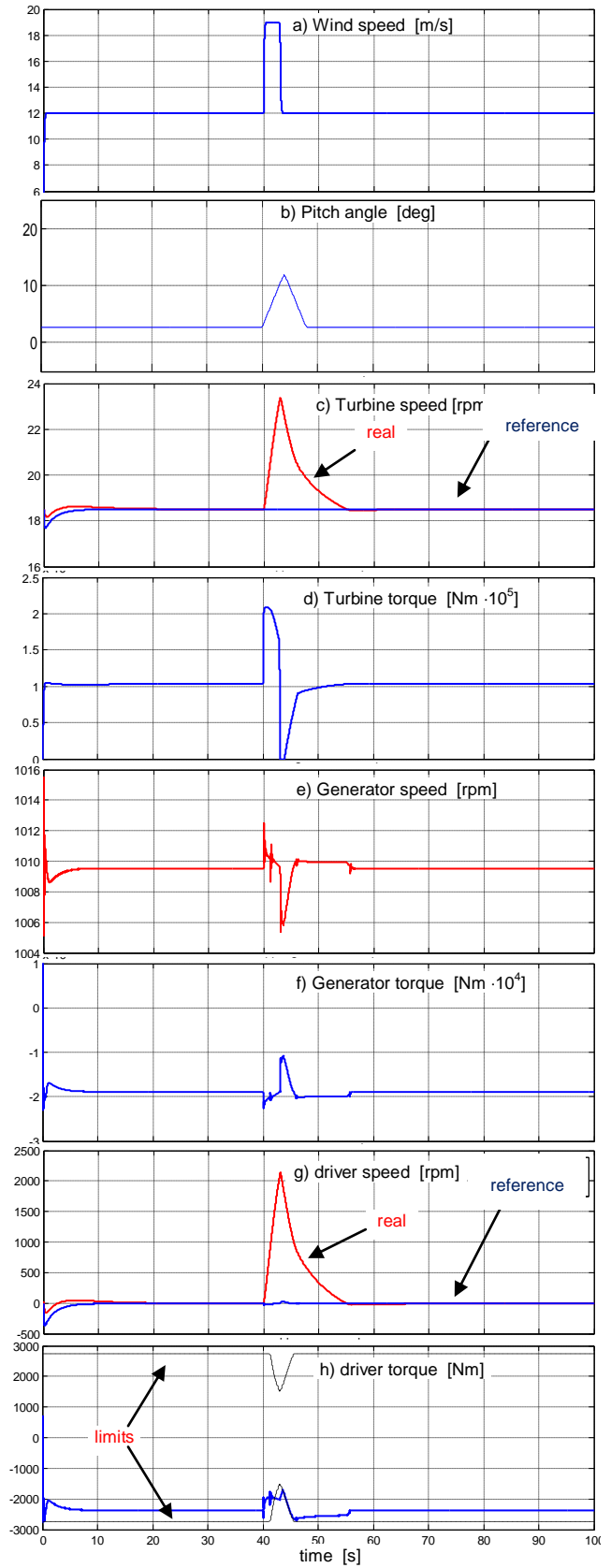


Fig. 11 WECS operation during wind gust 12 → 18 m/s
 a-d) turbine data; e-f) generator speed and torque; g-h) driver speed and torque.